M. Chen et al. (Eds.)

doi:10.3233/ATDE220447

Acoustic Metamaterials Composed of Pre-stressed Oscillator Unit Cells and the Effective Method of Adjusting and Expanding Bandgap

Yiliang MA [a], Xiaoming WANG [a] and Yulin MEI [b,1]
[a] *School of Mechanical Engineering, Dalian University of Technology, 116024 Dalian, China*
[b] *School of Automotive Engineering, Dalian University of Technology, 116024 Dalian, China*

Abstract. The bandgap adjustment and expansion is an important research direction in acoustic metamaterial fields. This paper designs a kind of acoustic metamaterial composed of periodically arranging oscillator unit cells, and proposes an effective way to adjust the central frequencies of the bandgap and widen the frequency range of the bandgap. First, we design an acoustic metamaterial unit cell constructed by the base structure, a mass block, and bending elastic beams connecting the mass block with the base structure; then, study the effect of pre-stresses applying to the bending elastic beams on the bandgap characteristics of the acoustic metamaterials composed of oscillator unit cells; finally, construct a kind of periodic acoustic metamaterial by combing three groups of oscillator unit cells with different pre-stresses, and realize the effective expansion of the bandgap. Our study shows that, this kind of periodic acoustic metamaterial has bandgap characteristics of low-frequency and broadband; applying pre-stresses to the bending elastic beams can make the bandgap shift towards low frequencies but will result in a narrow bandgap; combining oscillator unit cells with different pre-stresses can effectively widen the bandgap, overcoming the limitation of narrow bandgap due to applying pre-stresses.

Keywords. Acoustic metamaterials, local oscillators, pre-stresses, bandgap characteristics

1. Introduction

Reducing vibration and noise has always been a difficult problem in modern industry, especially for low frequency vibration and noise below 500Hz [1]. According to the mass density law, a large mass is needed to isolate low-frequency vibration, which is not applicable and even not possible in engineering [2]. Researching local resonance acoustic metamaterials is of great significance for low-frequency acoustic waves attenuation.

Liu et al. proposed locally resonant acoustic materials for the first time and clarified the acoustic characteristic adjustment mechanism of the materials [3], providing an approach to adjust low-frequency characteristics of small-scale acoustic materials by

[1] Yulin Mei, Corresponding author, School of Automotive Engineering, Dalian University of Technology, 116024 Dalian, China; E-mail: meiyulin@dlut.edu.cn.

exciting local resonance of resonating units. Wang et al. designed the tunable locally resonant acoustic metamaterials composed of the elastic matrix, metallic cores, and elastic beams connecting metallic cores to the elastic matrix, and realized the bandgap tunability through the buckling of the elastic beams [4]. Harne et al. manufactured the hyperdamping metamaterial with embedded inclusions in poroelastic host media, and analyzed the effect of the hyperdamping phenomenon caused by the resonant mode of embedded inclusions on broadband vibration attenuation and acoustic energy absorption [2]. Qin et al. designed a kind of acoustic metamaterial comprising buckling vibrator units embedded periodically into a continuous bar, and compared the bandgap characteristics of the acoustic metamaterials with different structural parameters and material parameters [5]. Domenico et al. simulated the in-plane elastic wave propagation in the locally resonant metamaterial comprising a regular grid of Swiss-cross holes, and observed several unusual wave phenomena in ultrasonic frequency regime, such as negative refraction and wave trapping [6].

This paper mainly addresses a kind of periodic acoustic metamaterial composed of oscillator unit cells, and provides an effective method of adjusting and expanding the bandgap by applying pre-stresses to oscillator unit cells and combining oscillator unit cells with different pre-stresses. The oscillator unit cell consists of a square base structure, a mass block, and four pairs of bending elastic beams connecting the mass block with the base structure. When the bending elastic beam is pre-stressed, its axial stiffness will reduce a lot, resulting in a shift of the natural frequencies of the unit cell towards low frequencies, thus the bending elastic beam can be regarded as a spring. The four pairs of bending elastic beams and the mass block construct an oscillator. When the stiffness of the oscillator decreases, although the bandgap moves towards low frequencies, the acoustic wave attenuation also decreases. How to determine the pre-stress applied to bending elastic beams and combine oscillator unit cells with different pre-stresses to construct periodic acoustic metamaterials with low-frequency broadband characteristics is a key problem the paper will focus on and solve.

2. Theoretical Models of Dispersion Relation and Bandgap Calculation

For non-uniform isotropic linear elastic materials, the wave equation is expressed by

$$\rho\ddot{\mathbf{u}} = (\lambda + \mu)\nabla(\nabla \cdot \mathbf{u}) + \mu\nabla^2\mathbf{u} \tag{1}$$

where, ρ is the material density; $\mathbf{u}$ the displacement; λ and μ are the medium's elastic constants; ∇ the Hamilton operator.

Considering the periodicity and symmetry of phononic crystals, based on Bloch's theorem, for a linear system with translational periodicity, its eigenfield has the form of Bloch function and can be written as

$$\mathbf{u}(\mathbf{r}) = \boldsymbol{u_k}(\boldsymbol{r})e^{ik\cdot r} \tag{2}$$

where k is the Bloch wave vector, and the amplitude function u(r) has translational periodicity. Substitute equation (2) into equation (1) to solve the wave equation and calculate corresponding eigenfrequency. The relationship between the eigenfrequency and the wave vector k is the energy band diagram of the phononic crystal.

Dispersion relation and frequency responses can describe elastic wave propagation in structures and the materials. This paper simulates an infinite structure model by imposing Floquent-Bloch periodic boundary conditions on the model boundary, and analyzes bandgap characteristics of the infinite model by solving eigenwave vectors *k*. Meanwhile, a finite periodic structure model is also built to calculate the frequency response by solving the steady-state vibration equation within a given frequency range.

3. Oscillator Unit Cell Model and Bandgap Characteristics

A 2D oscillator unit cell is designed and constructed by a square base, a mass block, and four pairs of bending elastic beams connecting the mass block to the square base, as shown in figure 1. The bending elastic beams are pre-stressed and embedded into the inner circle of the base to adjust the stiffness and modal frequencies of the oscillator. When the frequency of an incident elastic wave approaches to the mode frequencies of the oscillator, the incident wave will interact with the oscillator, resulting in local resonance of the oscillator and a low-frequency bandgap. The bending elastic beams connecting the base and the mass block make the oscillator have self-balancing properties when vibrating.

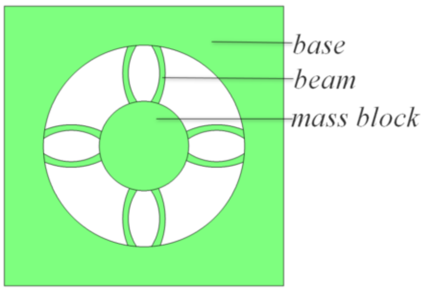

Figure 1. Oscillator unit cell.

It is assumed that the square base and bending beam are elastic polymers; the mass block is made of high-density lead; the unit cell's lattice constant is a=50mm; the radius of the mass block is R_0=18mm; the radius of curvature of the bending elastic beam is r=18mm; the radius of inner circle of the base is R_1=50mm. The material parameters of the oscillator unit cell are shown in table 1.

Table 1. Material parameters.

	Materials	Elastic Modulus (GPa)	Poisson's ratio	Density (kg/m^3)
Beam	TPO	20e-3	0.49	1140
Base	TPU	50e-3	0.49	1250
Mass block	lead	16	0.36	11370

Bandgap characteristics can evaluate sound absorption or vibration isolation of structures or materials. In this section, we simulate an infinite period structure by applying the Floquet periodic condition on the oscillator unit cell boundaries. The bandgap characteristics are analyzed and the eigenwave vectors are calculated. The energy band diagram describing the relationship between the wave vector $\boldsymbol{k}$ and the frequency is given in figure 2.

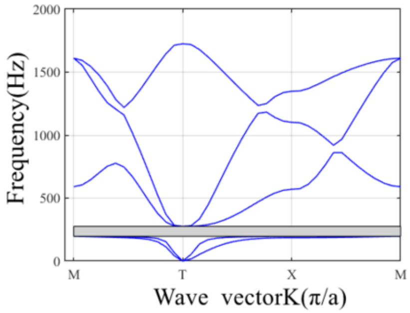

Figure 2. Energy band diagram (no pre-stresses).

It can be known from figure 2, at the resonance frequency of 234Hz, the oscillator mainly vibrates in the horizontal direction; within the frequency range of 234-350Hz, the oscillator couples with the incident wave so that there is no elastic wave propagating, forming a bandgap.

4. Effect of Pre-stresses on the Bandgap Characteristics

Bandgap adjustment and expansion has always been a key research issue in acoustic metamaterial fields, and adjusting or expanding bandgaps by geometric deformations is an important direction. In this paper, the pre-stress applied to the bending elastic beam is used to change stiffness of the oscillator and adjust bandgap characteristics of the period acoustic metamaterial composed of the oscillator unit cells. The pre-stress can be introduced to the bending elastic beams prior to assembly, or be loaded by screws fixing the bending elastic beam to the mass block and the base after assembly. The both methods of applying pre-stresses are easy to operate and are not expensive.

In order to research the effect of pre-stresses on center frequencies and frequency ranges of the bandgap, we simulate the energy band diagrams and the vibration modal diagrams. Figure 3 illustrates the bending elastic beams with different pre-stress magnitudes, including 0.00Mpa, 0.80Mpa, 1.00Mpa and 1.35Mpa.

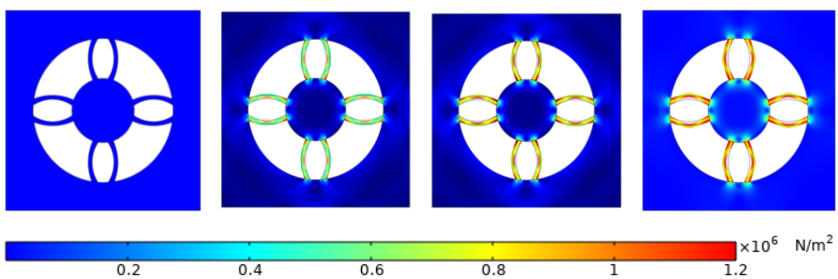

Figure 3. Bending elastic beams with different pre-stress magnitudes.

Figure 4 shows a stiffness variation curve of the oscillator with pre-stresses applied to bending elastic beams. Table 2 gives the first four modal frequencies under different pre-stress magnitudes. Figure 5 includes three energy band diagrams, corresponding to the pre-stress magnitudes equal to 0.80Mpa, 1.00Mpa and 1.35Mpa, respectively.

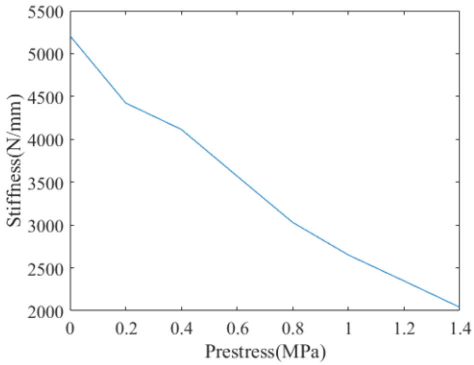

Figure 4. Stiffness variation curve of the oscillator with pre-stresses.

Table 2. Modal frequencies under different pre-stress magnitudes

Pre-stress (Mpa)	1st-order (Hz)	2nd-order (Hz)	3rd-order (Hz)	4th-order (Hz)
0.00	206	234	234	791
0.80	163	185	185	749
1.00	123	154	154	715
1.35	88	128	128	699

Figure 4 and table 2 indicate, with the increase in the pre-stresses applied to the bending elastic beams, the oscillator stiffness decreases significantly, and the mode frequencies of the oscillator also decrease greatly, such as the first-order frequency dropping from 206Hz to 88Hz, the second- and the third-order frequencies dropping from 234Hz to 128Hz.

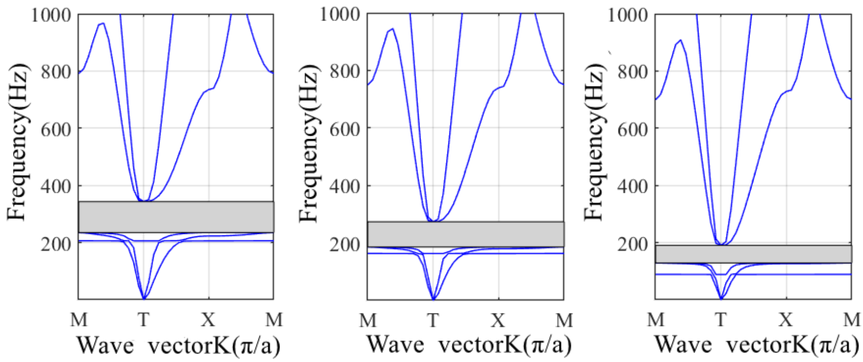

Figure 5. Energy band diagrams under the pre-stresses of 0.80Mpa, 1.00Mpa and 1.35Mpa.

In figure 5, it can be found that, with the increase of pre-stresses, the overall energy band curves shift to low frequencies. When the pre-stress is 1.35Mpa, the bandgap shifts from 234-350Hz to 128-180Hz, where 234-350Hz is the frequency range of the bandgap under no pre-stress case. Obviously, the pre-stress of 1.35Mpa makes the bandgap shift towards low frequencies, but it also results in a narrow bandgap due to the decrease in the oscillator stiffness.

Figure 6 gives the first four vibration modals of point X in Brillouin region while the pre-stress equal to 1.35Mpa. The modal diagrams show that, the first-order mode is a rotational mode at the frequency of 88 Hz, where the oscillator and the incident wave are not coupled and the bandgap cannot be opened; the second- and the third-order modes are localized resonance modes along the x or the y directions at the frequency of 128 Hz, where the oscillator couples with the incident waves so the energy of the incident wave is transmitted to the oscillator and is consumed by vibration; in the fourth-order mode, the vibrations mainly occur in the base and the bending elastic beams while the mass block is at rest.

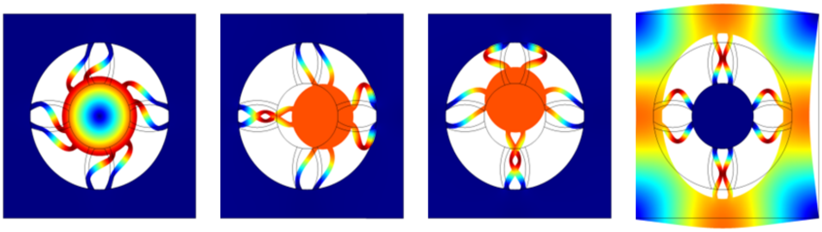

Figure 6. Vibration modal diagrams (the first four vibration modals).

In order to further observe the elastic wave propagation in the periodic acoustic metamaterial composed of oscillator unit cells, a finite periodic structure is built by periodically arranging the oscillator unit cells in the 2D plane, as shown in figure 7, and frequency responses are calculated by solving the steady-state vibration equation within a frequency range of 100-450Hz.

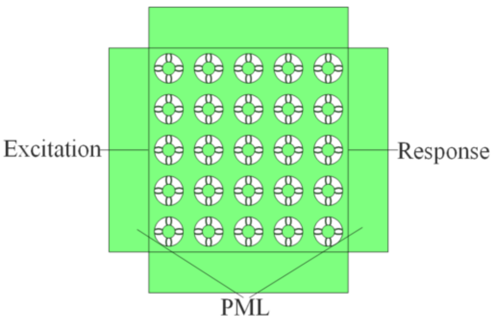

Figure 7. Acoustic metamaterial.

A point vibration is applied on the left, and displacement response is detected on the right side. The vibration isolation effect can be evaluated by

$$TL = 20 \cdot \log(|U_t|/|U_i|) \quad (3)$$

where, $|U_t|$ and $|U_i|$ are the amplitudes of transmitted wave and incident wave, respectively.

In figure 8, the frequency responses corresponding to different pre-stress magnitudes are shown. Because the simulation results of the pre-stress of 1.0MPa and 1.35MPa are very close, the curve corresponding to the pre-stress of 1.0MPa is not given in figure 8.

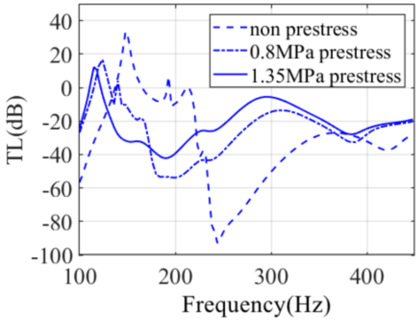

Figure 8. Frequency responses.

Under no pre-stress case, the bandgap over the attenuation of 30dB is 230-350Hz, and the maximum value is 90dB. While the pre-stress equal to 1.35Mpa, the bandgap is 138-218Hz, and the maximum is 40dB. It can be found that, after applying pre-stresses, the bandgap moves to low frequency but the bandgap width becomes narrow and the elastic wave attenuation reduces. The conclusions coincide with those drawn from energy band analysis of the infinite period structure.

5. Bandgap Combination

The above study shows that the adjustment of the bandgap of the periodic acoustic metamaterial composed of the oscillator unit cells can be achieved by applying pre-stresses to the bending elastic beams. But the problem is that, as the bandgap shifts towards low frequencies, the bandgap becomes narrow. In order to overcome the problem, we adopt a method of combining oscillator unit cells with different pre-stress magnitudes to extend the bandgap of the acoustic metamaterial.

Figure 9 shows a kind of low-frequency broadband acoustic metamaterial constructed by combining 3 groups of oscillator unit cells with different pre-stresses.

The first group consists of periodically arranging oscillator unit cells with the pre-stress of 1.35Mpa, responsible for attenuating elastic waves within the frequency range of 128-180Hz. The oscillator unit cells with the pre-stress of 0.8Mpa are selected to form the second group, responsible for attenuating elastic waves within the frequency range of 180-230Hz. The third group is composed of non-prepressed oscillator unit cells, responsible for attenuating elastic waves within the frequency range of 230-350Hz.

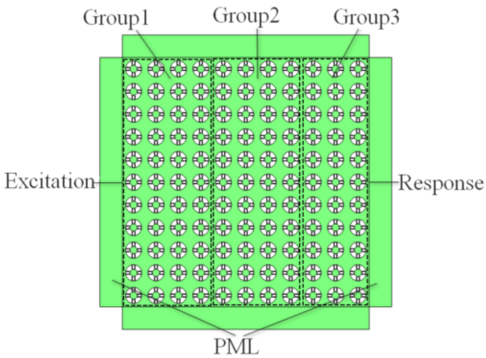

Figure 9. Acoustic metamaterial.

The frequency response is simulated to analyze the elastic wave propagation in the periodic acoustic metamaterial, as shown in figure 10.

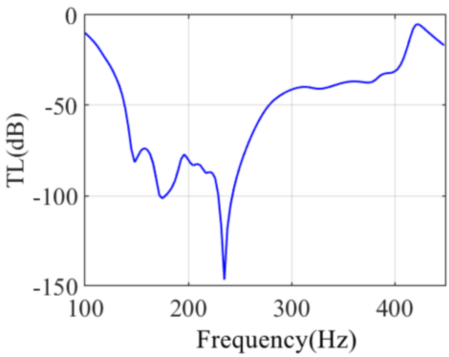

Figure 10. Frequency responses.

It can be found that, the bandgap with TL above 30dB spans a frequency range of 138-376Hz, about 2 times of the bandgap width of the acoustic metamaterial composed of non-prepressed oscillator unit cells; there are 3 local minima at 138Hz, 170Hz and 234Hz, which are equal to or approximate to the modal frequencies of oscillator unit cells with the pre-presses of 1.35Mpa, 0.80Mpa and 0.00Mpa, indicating that oscillator unit cells with the different pre-stresses absorb the elastic waves in different frequency ranges. In figure 10, the average TL can reach 60dB, showing good attenuation performances of the acoustic metamaterial. Furthermore, for the sake of conveniently observing the vibration of the oscillator unit cells, the displacement diagrams of the middle row composed of 11 oscillator unit cells are shown in figure 11, where the three displacement diagrams are obtained at different frequencies.

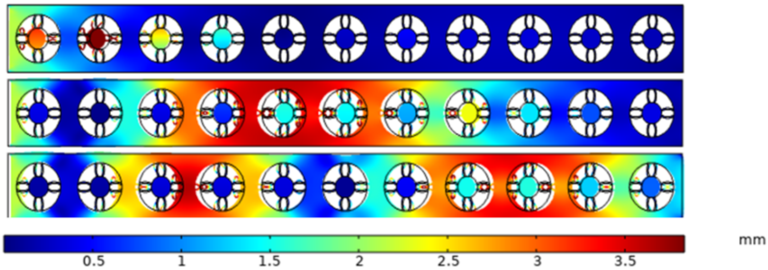

Figure 11. Displacement diagrams at 140Hz, 200Hz and 300Hz.

In figure 11, the top displacement diagram is obtained at the frequency of 140Hz, and it can be found that, only the first group of oscillator unit cells vibrates and absorbs elastic waves while the other two groups hardly vibrate. The middle displacement diagram corresponds to 200Hz, where the first group vibrates very little and the elastic waves are mainly absorbed by the vibration of the second group of oscillator unit cells. In the bottom displacement diagram corresponding to 300Hz, only the third group vibrates and absorbs energy. The simulation results show that combining oscillator unit cells with different pre-stresses is an effective method of adjusting and expanding the bandgaps of the periodic acoustic metamaterial.

6. Conclusions

This paper designs a kind of acoustic metamaterial composed of periodically arranging oscillator unit cells, which has bandgap characteristics of low frequency and broadband; proposes an effective way to adjust the center frequency of the bandgap by applying pre-stresses to the oscillator unit cells; and implements the frequency range expansion of the bandgap by combing different oscillator unit cells. The main conclusions are as follows:

- Applying pre-stresses to the bending elastic beam in the oscillator unit cell can make the bandgap shift towards low frequencies, but will narrow the frequency range of the bandgap and reduce acoustic wave attenuation;
- Combining oscillator unit cells with different pre-stresses can effectively widen the bandgap, overcoming the limitation of narrow bandgap due to applying pre-stresses to the bending elastic beams;
- Properly adjusting pre-stresses applying to oscillator unit cells and combining oscillator unit cells with different pre-stresses can be adopted together to design the acoustic metamaterial with bandgap characteristics of low frequency and broadband, which is easy to implement in engineering.

Acknowledgment

This research was financially supported by the National Science Foundation No.51975083, No.51775080, No.11372059 and No.11272073.

References

[1] Wu JH, Ma FY, Zhang SW, et al. Review on the application of acoustic metamaterials in low frequency vibration and noise reduction. Chinese Journal of Mechanical Engineering. 2016; 52(13):68-78.
[2] Harne RL, Yu S, Dai Q. Trapping and attenuating broadband vibroacoustic energy with hyperdamping metamaterials. Extreme Mechanics Letters. 2017; 12:41-47.
[3] Liu Z, Zhang X, Mao Y, et al. Locally resonant sonic materials. Science. 2000; 289(5485):1734-1736.
[4] Wang P, Casadei F, Shan S, et al. Harnessing buckling to design tunable locally resonant acoustic metamaterials. Physical Review Letters. 2014; 113(1):014301.
[5] Qin SH, Wang XM, Mei YL. A design method of acoustic metamaterials with buckling vibrators. Journal of Physics: Conference Series. 2020; 1605(012097): 1-10.
[6] Domenico Tallarico, Stewart G. Haslinger. Trapped modes and negative refraction in a locally resonant metamaterial: Transient insights into manufacturing bounds for ultrasonic applications. Applied Sciences-Basel. 2021; 11(16): 1-15.